Real-Time Octree Generation from Rotating Objects

Richard Szeliski

Digital Equipment Corporation

Cambridge Research Lab

CRL 90/12 December 21, 1990

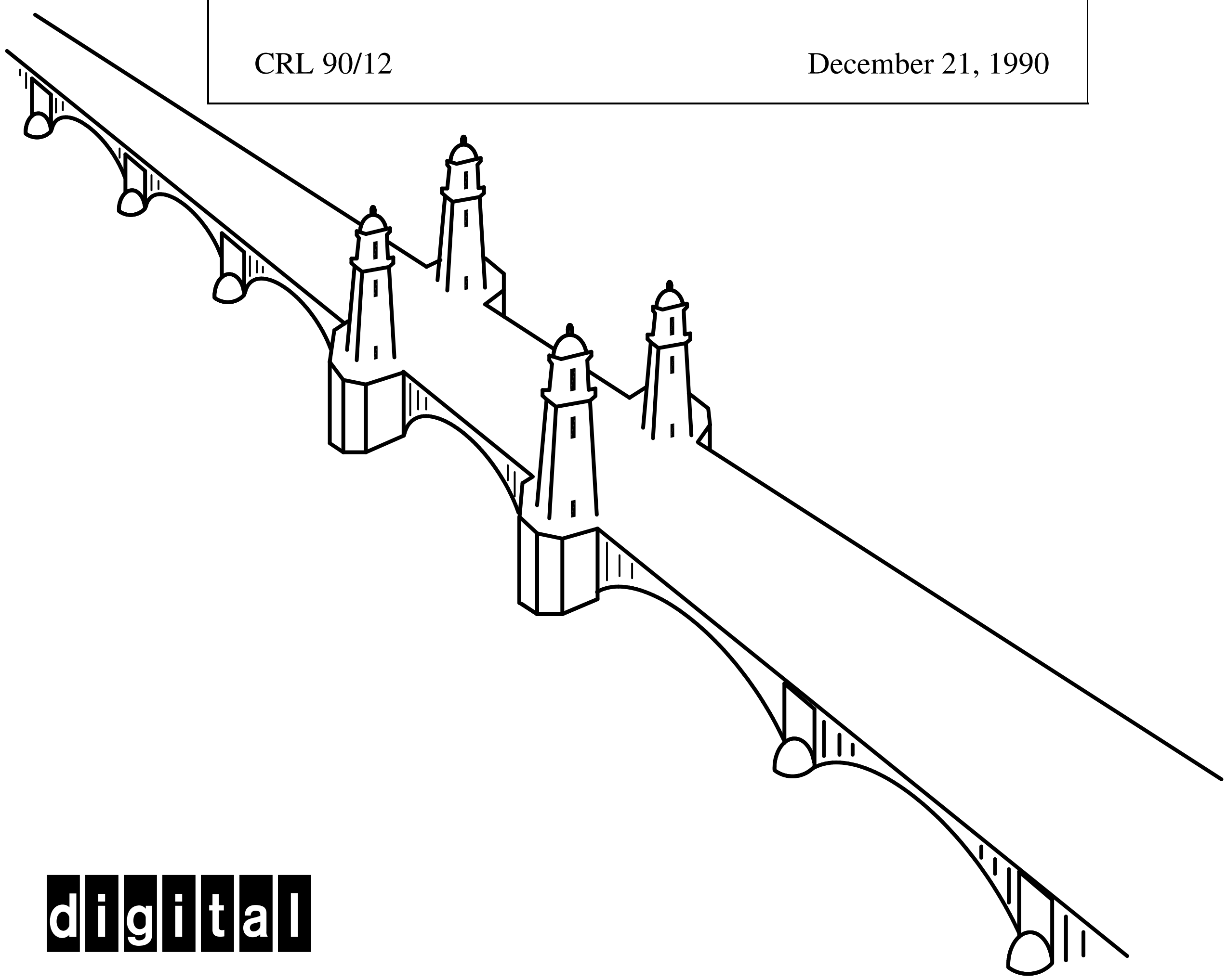

digital

CAMBRIDGE RESEARCH LABORATORY

Technical Report Series

Digital Equipment Corporation has four research facilities: the Systems Research Center and the Western Research Laboratory, both in Palo Alto, California; the Paris Research Laboratory, in Paris; and the Cambridge Research Laboratory, in Cambridge, Massachusetts.

The Cambridge laboratory became operational in 1988 and is located at One Kendall Square, near MIT. CRL engages in computing research to extend the state of the computing art in areas likely to be important to Digital and its customers in future years. CRL's main focus is applications technology; that is, the creation of knowledge and tools useful for the preparation of important classes of applications.

CRL Technical Reports can be ordered by electronic mail. To receive instructions, send a message to one of the following addresses, with the word **help** in the Subject line:

On Digital's EASYnet:	CRL::TECHREPORTS
On the Internet:	techreports@crl.dec.com

digital™

Cambridge Research Laboratory
One Kendall Square
Cambridge, Massachusetts 02139

Real-Time Octree Generation from Rotating Objects

Richard Szeliski

Digital Equipment Corporation

Cambridge Research Lab

CRL 90/12 December 21, 1990

Abstract

The construction of a three-dimensional object model from a set of images taken from different viewpoints is an important problem in computer vision. One of the simplest ways to do this is to use the silhouettes of the object (the binary classification of images into object and background) to can construct a bounding volume for the object. To efficiently represent this volume, we use an octree, which represents the object as a tree of recursively subdivided cubes. We develop a new algorithm for computing the octree bounding volume from multiple silhouettes, and apply it to an object rotating on a turntable in front of a stationary camera. The algorithm performs a limited amount of processing for each viewpoint, and incrementally builds the volumetric model. The resulting algorithm requires less total computation than previous algorithms, runs in real-time, and builds a model whose resolution improves over time.

Keywords: Computer vision, 3-D model construction, image sequence (motion) analysis, volumetric models, octrees, silhouettes, computer aided design, computer graphics animation.

Contents

1 Introduction

This paper describes a new approach to creating 3D models of objects from multiple views. In our scenario, an object rotates on a turntable in front of a static camera. We use only the silhouettes—the binary classification of each image into object and background—to compute a bounding volume for the object. This algorithm enables us to obtain a quick and rough model of the object in real-time. This model can be used in conjunction with a more sophisticated shape-from-motion algorithm that relies on the detailed analysis of optic flow, which is presented in a companion report [Szeliski, 1990]. In this context, it serves both as an initial model for shape refinement, and as a non-linear (bounding volume) constraint on the final shape.

The automatic acquisition of 3-D object models is important in many applications. These include robotics manipulation, where the object must first be described and/or recognized before it can be manipulated; Computer Aided Design (CAD), where automatic model building can be used as an input stage to the CAD system; and computer graphics animation, where it can facilitate the task of an animator by giving him easy access to a large catalog of real-world objects. All of these applications become much more interesting if the acquisition can be performed quickly and without the need for special equipment or environments.

The problem of building octree models from multiple views has a long history in the computer vision field. Octrees were first introduced as an efficient representation for geometric models by Jackins and Tanimoto [1980] and Meagher [1982] (see also [Carlbom *et al.*, 1985]). A good survey of octree representations can be found in [Samet, 1989], and a survey of construction and manipulation techniques in [Chen and Huang, 1988].

The construction of volumetric description from multiple views was first described by Martin and Aggarwal [1983] (the representation used was a collection of "volume segments"). Chien and Aggarwal [1986b] constructed an octree from three orthographic projections. This approach was extended to 13 standard orthographic views by Veenstra and

Ahuja [1986]. Hong and Shneier [1985] and Potmesil [1987] both used arbitrary views and perspective projection. In both of these papers, an octree of the conic volume formed by the silhouette and the center of projection is computed for each viewpoint, and the octrees from all of the viewpoints are then intersected. Both approaches project the octree cubes into the image plane to perform the object/silhouette intersection. In contrast to this, Noborio *et al.* [1988] and Srivastava and Ahuja [1990] perform the intersections in 3-space, which eliminates the need for perspective projection. Both of these approaches use a polygonal approximation to the silhouette. Additional research has also been done on building octrees from range data [Chien *et al.*, 1988] and the recognition of object models from octrees [Chien and Aggarwal, 1986a].

The new approach described in this paper was designed with two goals in mind: to process each image as it arrives (real-time), and to produce a coarse model quickly and refine it as more images are seen (incremental). A secondary goal of this research is to find highly parallelizable algorithms. Our approach is similar to Potmesil's [1987], but instead of building a separate octree for each view, we intersect each new silhouette with the existing model. More importantly, we do not build a full-resolution octree after each view. Instead, we build a coarse octree description first, and then refine it as the object continues to rotate in front of the camera. This makes our approach similar to other recent incremental algorithms [Matthies *et al.*, 1989]. As we will see, this approach significantly reduces both the individual computation per image and the total computation performed, since less cubes are generated and tested.

Our approach also uses a very efficient 2-D image plane intersection test based on bounding squares and the chess-board distance transform [Rosenfeld and Kak, 1976] (Potmesil uses a quadtree or non-overlapping rectangle description). The 3-D projection operations, computation of the distance transform, and bounding box intersection test are easily parallelizable, and can thus take advantage of modern massively parallel architectures. The 3-D perspective projection is also well suited to graphics accelerators [Clark, 1982] or fast floating-point microprocessors.

We begin the paper in Section 2 with a brief review of the octree representation. In Section 3, we describe how our algorithm hierarchically constructs an octree. In Section 4, we describe our fast image plane intersection test. In Section 5, we show some results of our algorithm operating on synthetically generated images. We analyze the complexity of our algorithm in Section 6. In Section 7, we switch gears and discuss a number of practical image processing issues: silhouette computation (adaptive thresholding), the automatic determination of turntable position, and the calibration of the camera position. This leads up to some results obtained from real images (Section 8). In Section 9, we discuss a number of extensions, including moving the camera and repositioning the object on the turntable. We close in Section 10 with a comparison between our new algorithm and other approaches.

2 Octree models of shape

An octree is a tree-structured representation that can be used to describe a set of binary valued volumetric data enclosed by a bounding cube. The octree is constructed by recursively subdividing each cube into eight sub-cubes, starting at the root node (a single large cube). Each cube in an octree can be one of three *colors*. A *black* node indicates that the cube is totally occupied (all of its data = 1), and a *white* node indicates that it is totally empty (all of its data = 0). Both black cubes and white cubes are leaf nodes in the tree. A *gray* cube lies on the boundary of the object and is only partially filled. It is an interior node of the tree and has eight equally sized children of different colors. Figure 1a shows a graphical view of a small octree, and Figure 1b shows its associated colored tree representation.

Octrees are an efficient representation for most volumetric objects since there is a large degree of coherence between adjacent *voxels* (volume elements) in a typical object. A number of schemes have been developed to efficiently represent and encode octrees [Chen and Huang, 1988]. For our application, we use a very simple representation where all of the

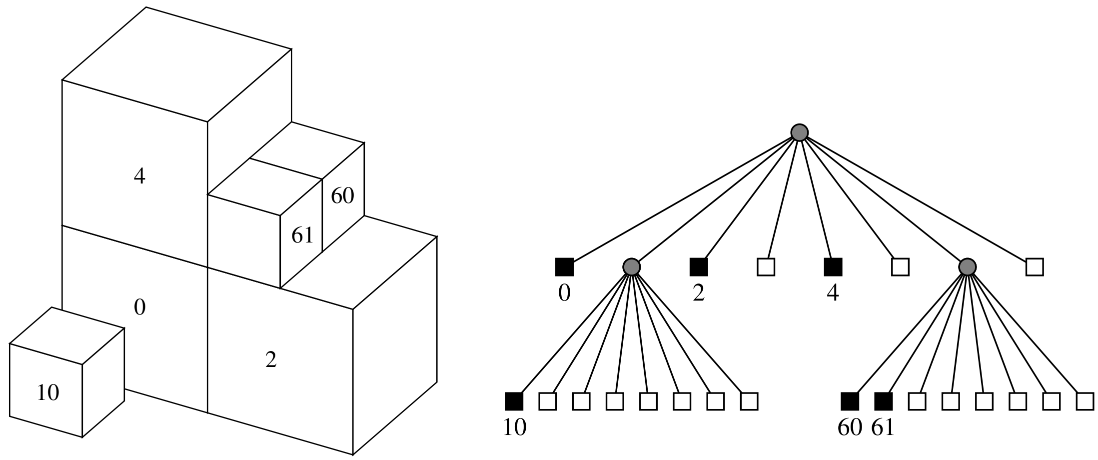

Figure 1: A simple two-level octree and its tree representation

cubes at a given resolution level are kept in the same array. Each cube explicitly represents its x, y, and z coordinates, as well as its color and a pointer to the first of its children (for a gray cube). This representation is well suited to the commonly occurring operations in our algorithm. In particular, it enables the fast projection into the image of all the cubes at a given resolution level.

3 Hierarchical octree construction from multiple views

Our basic algorithm constructs the octree in a hierarchical coarse-to-fine fashion. For a given octree resolution, the inner loop of the algorithm carves out a 3D volume incrementally from a sequence of silhouettes. After one complete revolution of the object, those cubes whose color is still uncertain are subdivided. Because the octree is completely constructed at one resolution before refining the next one, a minimum of extra cubes that eventually get trimmed off are created.

In more detail, we start each new revolution of the object on the turntable with a collection of black cubes all at the given (finest) resolution level; to initialize the algorithm, we start either with a single black cube, or with a small collection (e.g., $8 \times 8 \times 8$) of black cubes. Cubes that are black are believed to lie completely within the object, white cubes are known to lie outside of the object, and gray cubes are ambiguous (this is different from the usual octree coloring scheme, where gray cubes are known to have children of differing colors). For each new image that is acquired, we project all of the current cubes into the image and test whether they lie totally within or outside of the silhouette (Section 4). We then update the color of each cube according to the following table:

old color ⇒ *test result* ⇓	black	gray	white
inside	black	gray	white
ambiguous	gray	gray	white
outside	white	white	white

Note that cube colors can only change from black to gray or white, or from gray to white (i.e., the volume is "carved away").

For our hierarchical approach to work, the tests of projected cubes against the silhouettes can be crude, but they must not classify a cube as wholly inside or outside unless this is certain. Projected cubes that are erroneously classified as "ambiguous" will be colored gray (unless they are already white), and the decision as to their true color will be deferred to the next finer resolution level. This allows our intersection tests to be more sloppy and also makes our algorithm more robust against noise.

After one resolution level has been processed completely, i.e., the object has been seen from all of its views (which usually corresponds to a complete revolution), we refine the gray cubes by splitting them into eight pieces. The new cubes are initially colored black and are then processed as were the cubes at the previous resolution level. Note that since all of the possible views are used before proceeding to the next level, there is no need to update nodes that belong to levels coarser than the one currently being analyzed. If we wish to save storage space, we can go back later and compact the octree by converting gray nodes into black or white nodes if all of their children are the same color.

4 Image silhouette intersection tests

To make the above approach practical, we must have an efficient way to project the octree cubes into image-space coordinates and to test for intersection with the object silhouette. The perspective projection step is not a critical computational bottleneck, since it is trivially parallelizable, and specialized hardware exists to perform it [Clark, 1982]. In our current implementation, we simply project all eight corners of each cube using floating point arithmetic.

An opaque cube projected into the image plane will in general form a six-sided polygon. Performing an accurate test of this hexagon against the silhouette (which we represent as a binary image) can be quite time consuming. Instead, we use a coarser test based on the hexagon's bounding box, which may sometimes fail to detect a true inclusion or exclusion. This is acceptable in our overall framework, since this kind of "mistake" simply colors a cube gray, thus deferring the decision to the next finer resolution level.

More precisely, each projected cube is converted into a *bounding square*. This allows us to do the inclusion and exclusion tests using a single lookup into two distance maps constructed from the silhouette and its complement. These distance maps are one-sided versions of the chess-board distance transform [Rosenfeld and Kak, 1976]. Each point in the distance map contains the size of the largest square starting at that pixel that fits completely within the silhouette (Figure 2). These *half-distance transforms* for the silhouette and its complement can be computed using a single raster-scan pass over the image, or using an $O(\log d)$ step parallel algorithm, where d is the diameter of the largest region in the silhouette (Appendix A).

One final minor detail which must be resolved is how to compute the bounding square from the bounding box of the projected cube (which is defined by the minimum and maximum projected x and y values). We could center the bounding square over the bounding box, or push it flush left or right (top or bottom) against the bounding box. We

.	.	.	.	.	.	.	.	.	.
.	.	1	1	1	1	.	.	.	.
.	.	1	1	1	1	1	1	.	.
.	1	1	1	1	1	1	1	.	.
.	1	1	1	1	1	1	1	.	.
.	1	1	1	1	1	1	1	1	.
.	1	1	1	1	1	1	1	1	.
.	.	1	1	1	1	.	.	.	.
.	.	.	.	.	.	.	.	.	.

0	0	0	0	0	0	0	0	0	0
0	0	1	1	1	1	0	0	0	0
0	0	2	2	2	1	1	1	0	0
0	1	3	3	2	2	2	1	0	0
0	2	4	3	3	3	2	1	0	0
0	3	4	4	4	3	2	1	1	0
0	4	5	5	4	3	2	2	1	0
0	0	4	3	2	1	0	0	0	0
0	0	0	0	0	0	0	0	0	0

Figure 2: The half-distance transform and its use in inclusion testing. A sample binary image is shown on the left, and its half-distance transform on the right. The circled 5 in the distance map indicates that a 5×5 square is the largest square inside the silhouette whose lower left corner is at that pixel.

have chosen the latter approach, testing both bounding squares for possible inclusion or exclusion, since this will more often result in a successful test.

5 Synthetic model results

To determine the viability of our new algorithm and to quantify its performance, we decided to first test it on a series of synthetically generated images. Our test models were constructed by combining superquadric parts [Pentland, 1986; Solina and Bajcsy, 1990]. The models were rendered from a variety of viewpoints using a 3-D graphics modeling system. The rendered images, along with the simulated turntable orientation and camera position, were then given to the octree building program. The complete simulation system was run on-line, which enabled the observation of the simulated input images and resulting octree models simultaneously.

Figure 3 shows four of the superquadric models that we used. Figure 4 shows the corresponding octree models constructed from 32 evenly spaced views (11° increments). For these simulations, the camera was at 4.0 (times the cube size) from the object center, the inclination (from horizontal) was 20°, and the field of view was 30°. The octrees shown are rendered at 32^3 resolution, even though they were computed to 64^3 resolution. As we can see from these examples, the shape of these objects is recovered fairly well, although there are occasional "bulges" on some flats sides of the objects (due to a limited number of viewpoints) or at the top (unavoidable from this camera position).

To obtain a more quantitative measure of the algorithm's performance, we counted the number of cubes of each color created at each resolution level. As we can see from Table 1, at the finer levels, roughly 25% of the cubes are black, 25% are white, and 50% are gray. Since each gray cube gets split into eight children, the number of cubes roughly quadruples at each level. This is consistent with Meagher's [1982] finding that the number of cubes is proportional to the object surface area (measured in units of the finest resolution).

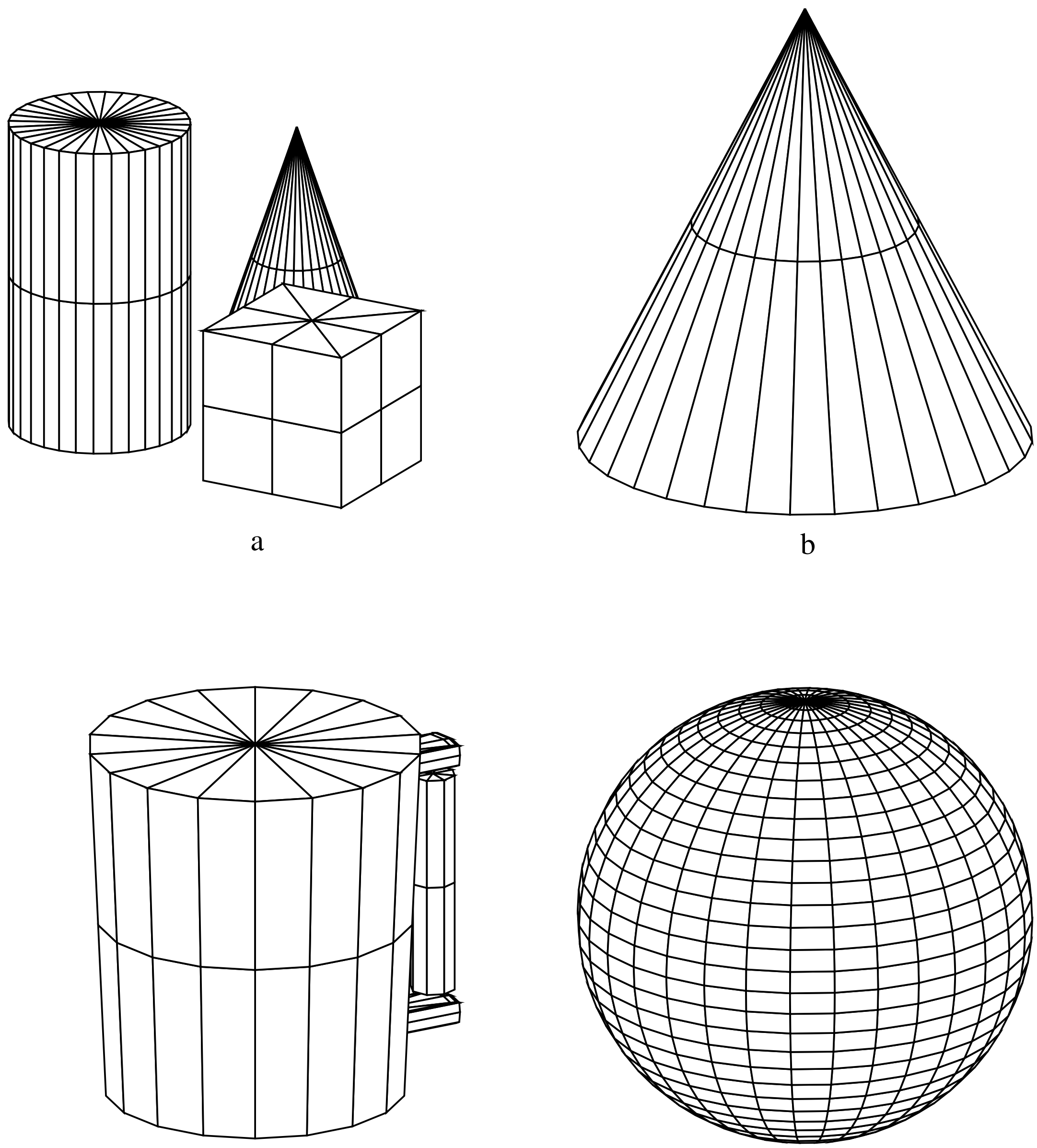

Figure 3: Superquadric test models: (a) blocks (b) cone (c) cup (d) sphere.

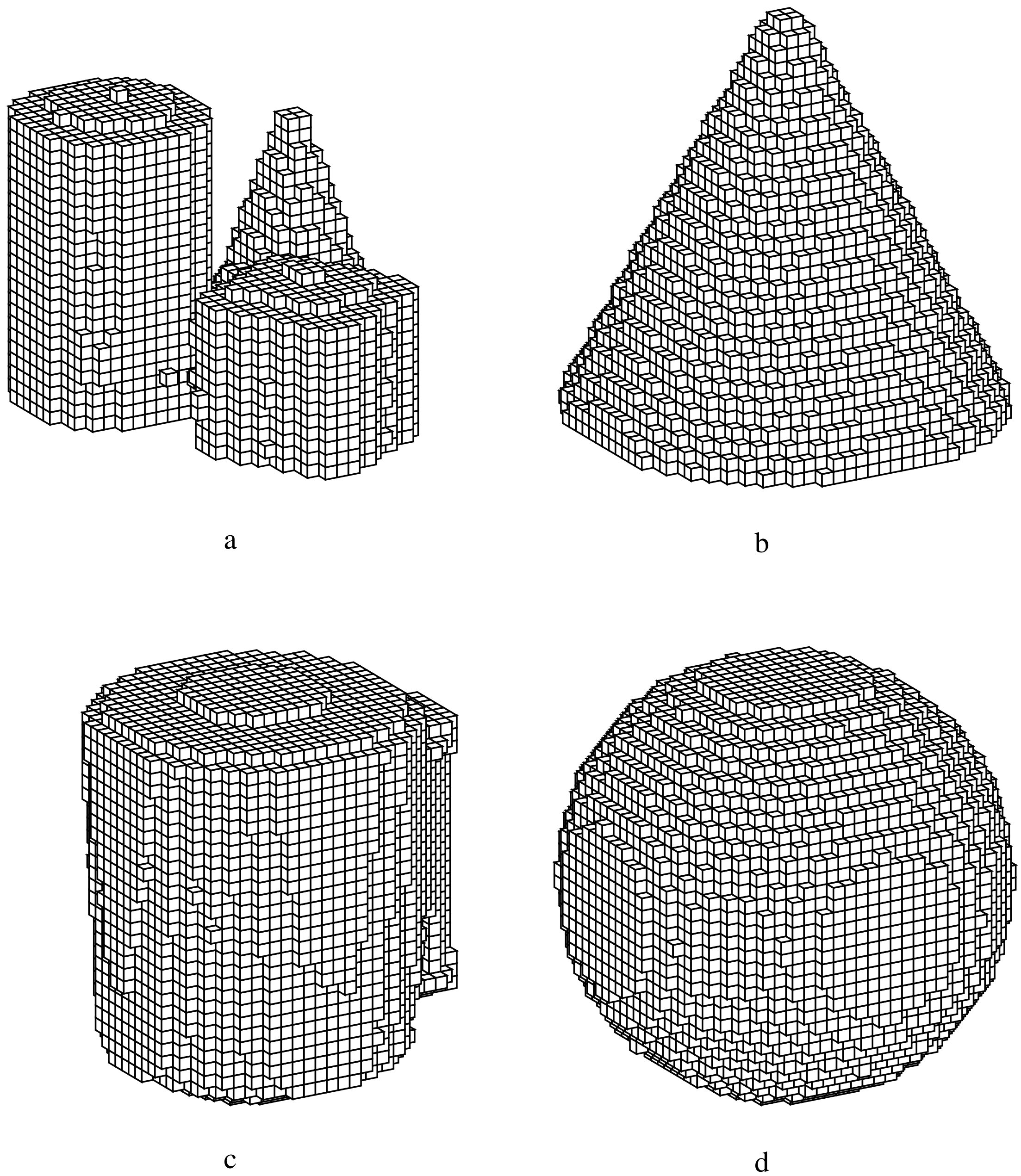

Figure 4: Derived octree models: (a) blocks (b) cone (c) cup (d) sphere.

We can verify if this is true by computing the surface area of each of the test objects (Table 2). Note that the flat areas at the bottom of the objects do not contribute significantly to the octree cube count, but do add significantly to the surface area. To verify the "accuracy" of our octree construction, we can compare the total volume of the octree with that of the original synthetic model (Table 2), as was done in [Veenstra and Ahuja, 1986; Potmesil, 1987; Srivastava and Ahuja, 1990]. For most of the volumes, these figures compare favorably, despite the restricted range of viewpoints.

6 Complexity analysis

The hierarchical octree construction algorithm developed in this paper is designed to operate in close to real-time. It should therefore perform less computation for each image acquired than previous approaches such as Potmesil's, and hopefully perform less computation in total. In practice, this is what occurs, because instead of building a complete octree from each image, only those cubes already on the surface of the model are refined.

As we saw previously, the expected number of cubes for an octree is proportional to its surface area (for a sufficiently smooth object). For most objects, this should be smaller than the surface area of the viewing cone formed by the camera and the object silhouette. To see if this occurs in practice, we can count the number of cubes in the octrees formed from a single silhouette (Table 3), which tells us the number of cubes in a viewing cone. Compared to the octree cube count from our hierarchical octree algorithm (Table 1), we see that the single-view count generally exceeds the 32-view count. The exception is for large simple objects that fill most of the octree volume.

This comparison only gives us a rough idea of the computation performed by both the hierarchical approach and the previous single resolution methods. For our hierarchical algorithm, the amount of processing required is proportional to the number of cubes at the current finest level, since only these cubes need to be projected and to have their color

model	number of cubes (%black/%gray)				
	level 2	level 3	level 4	level 5	level 6
blocks	64 (0/61)	312 (7/64)	1600 (13/56)	7152 (15/46)	26520 (18/48)
cone	64 (0/75)	384 (16/50)	1536 (16/50)	6176 (21/52)	25696 (23/50)
cup	64 (0/97)	496 (16/45)	1792 (19/56)	8040 (20/54)	34560 (22/50)
sphere	64 (13/88)	448 (16/61)	2176 (21/57)	9888 (24/52)	41248 (25/51)

Table 1: Cube counts for octrees computed from synthetic models (32 views)

model	cube count	analytic area	octree volume	analytic volume
blocks	35648	2.3844	0.1685	0.1552
cone	33856	2.5321	0.2643	0.2601
cup	44952	2.9734	0.3445	0.3102
sphere	53824	3.1278	0.5267	0.5190

Table 2: Total cube counts, surface area, and volumes for octrees

model	number of cubes (%black/%gray)				
	level 2	level 3	level 4	level 5	level 6
blocks	64 (0/83)	424 (21/63)	2120 (23/55)	9376 (25/52)	39232 (26/51)
cone	64 (11/78)	400 (25/56)	1800 (25/53)	7568 (26/51)	30672 (26/50)
cup	64 (22/78)	400 (33/53)	1680 (26/53)	7088 (26/50)	28376 (26/50)
sphere	64 (28/72)	368 (35/56)	1656 (29/53)	6984 (29/49)	27376 (26/50)

Table 3: Cube counts for octrees computed from synthetic models (single view)

updated. For the older octree algorithms, we must first construct an octree corresponding to the new view (in time proportional to the total number of cubes in all of the levels of Table 3), and then intersect this tree with the previously estimated object tree. The intersection algorithm ends up creating and deleting cubes all over the octree hierarchy, which makes its implementation on a parallel machine much more difficult.

Compared to the older octree intersection algorithms, our new hierarchical approach results in a much simpler and more parallelizable algorithm. For scenes of moderate to high complexity, it can result in dramatically lower computation (both per frame and overall) because the complete viewing cones arising from the silhouettes are not constructed. To better compare the performance of our new technique with the old approach, we will have to implement the intersection of viewing cones algorithm, which we have not yet done.

7 Image Preprocessing

Before we can apply our shape from silhouette algorithm to real image sequences, we must first address a number of low-level processing and calibration issues. These include the silhouette computation (object/background segmentation), the determination of turntable rotation, and the calibration of camera position.

7.1 Adaptation and thresholding

To compute the silhouette, we first adapt the imaging system to the background scene without the object by acquiring a few dozen images and computing the minimum, maximum, mean, and variance values at each pixel. With our current setup, we can perform this computation in near real-time (0.6 frames/second). These measurements are then used to precompute a range of normal values for each background pixel. When thresholding the image, any pixel falling outside of this range is assumed to be part of the object.

This adaptation stage is also used for a second purpose. To facilitate the automatic estimation of turntable rotation, we attach a black-and-white binary-coded strip onto the edge of the turntable (Figure 5 and Appendix B). During the adaptation stage, we allow the turntable to turn at its natural speed. For each pixel that is part of this position coding ring, we see both the black and white values. Because of the larger than usual variance, we can classify these pixels as part of the position encoding system and select a good threshold for each binary code pixel. The thresholding stage that computes the object silhouette thus classifies each image into four categories: black binary code, white binary code, background, and object (Figure 6).

7.2 Orientation estimation

To estimate the current orientation (rotation angle) of the turntable, we look at the binary code pixels in the classified image. We choose a small number of columns (currently 32) horizontally centered around the middle of the image, and in each column find the widest strip of adjacent binary code pixels. We then find the 8-bit binary code corresponding to the pixels in this strip (for now, by simply choosing 8 equally spaced samples within the strip),

Figure 5: Input image of object (cup), turntable, and position coding ring

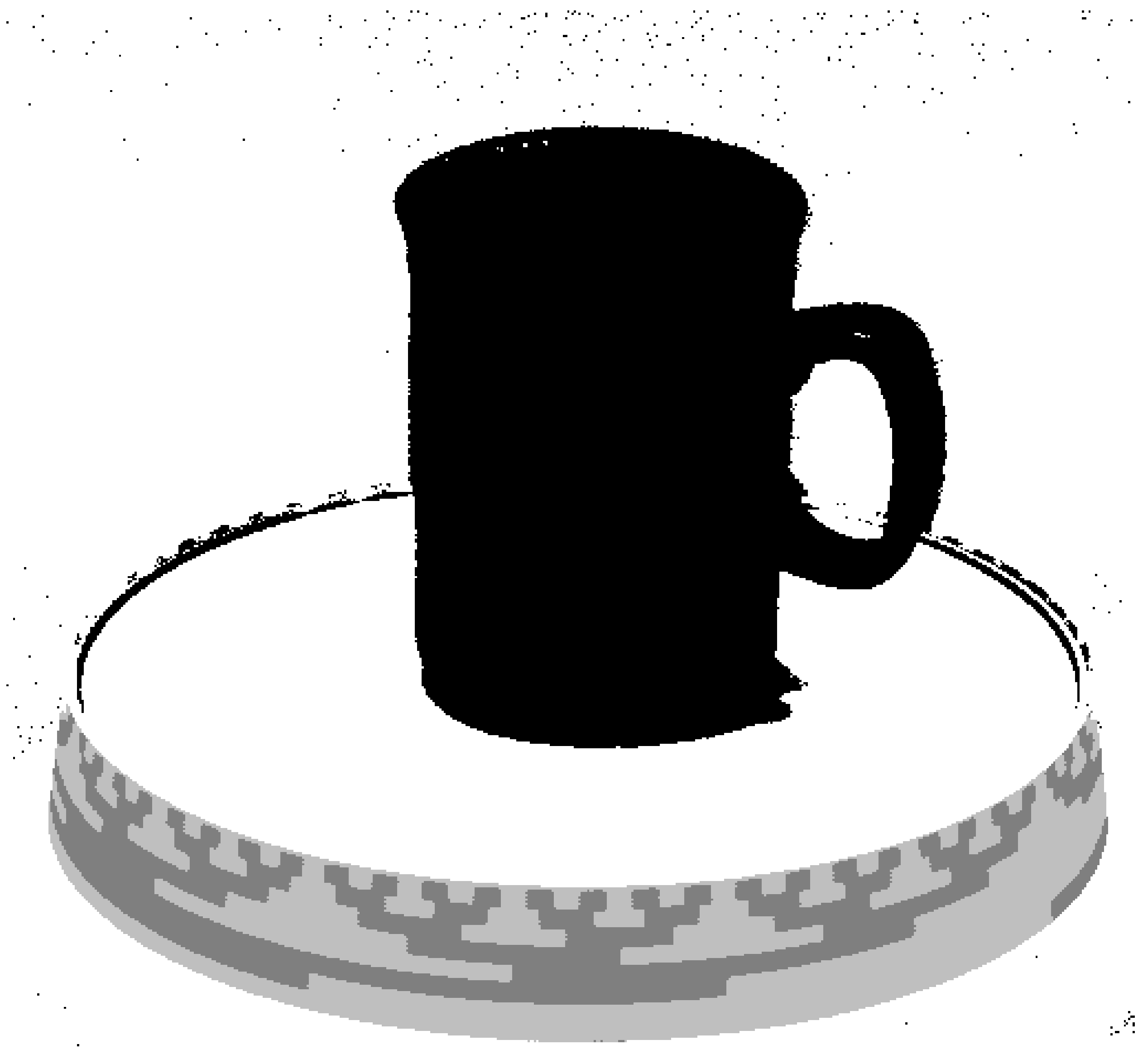

Figure 6: Thresholded image: black binary code = dark gray, white binary code = light gray, background = white, object = black.

and convert it into a value between 0 and 255. The sequence of binary patterns follows a Gray code, since only one bit changes at a time. This prevents an inconsistent code from arising from several bits changing asynchronously (which may occur due to camera noise or if the binary code is not perfectly vertical in the image). The binary values from all of the columns are averaged to obtain a position estimate that has better than 8-bit resolution (about $0.1°$ accuracy). This number, normalized to a 0° to 360° range, is the output of our turntable position estimator.

7.3 Camera parameter calibration

Before the object acquisition system can be run, we must determine the camera parameters, i.e., the camera position, orientation, and focal length. We do this using a known reference model placed on the turntable (Figure 7a) [Caprile and Torre, 1990]. First, we extract the edges by finding the zero crossings in the band-pass filtered image and using the gradient of the filtered image to compute the edge orientations and to throw away weak edges (Figure 7b). Next, we use the Hough transform with gradient directions [Ballard and Brown, 1982] to find the straight lines in the image (Figure 7c). Finally, these lines are used to compute the camera parameters relative to the reference cube [Caprile and Torre, 1990].

To compute the camera parameters relative to the center of rotation of the turntable (which is our desired object-centered coordinate frame), we must look at the reference cube from a number of viewpoints (i.e., while the cube is rotating on the turntable). We could at this stage also use Sawhney's [1990] method for simultaneously computing the cube structure and the cube rotation to do our calibration. Since we have not yet implemented this portion of our calibration procedure, we use a simpler method. We measure the camera distance to the object by hand and then compute the other camera parameters from the major and minor axes of an ellipse fitted to the image of the turntable top. This simplified method does not require a known reference model, only the knowledge of the turntable diameter.

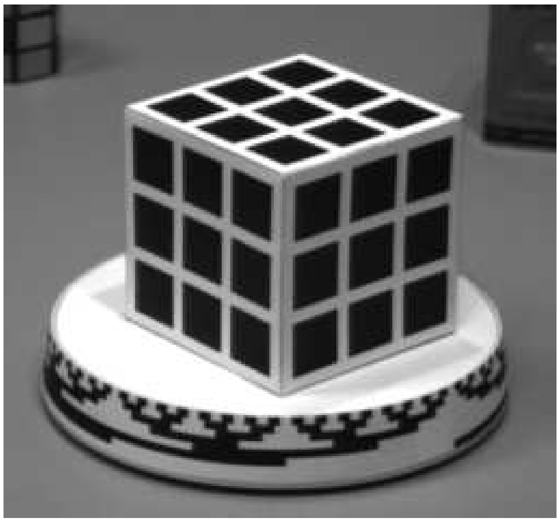

a

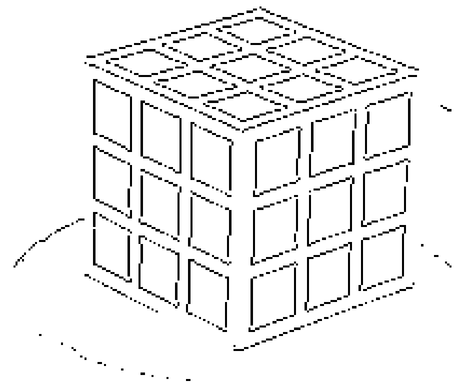

b

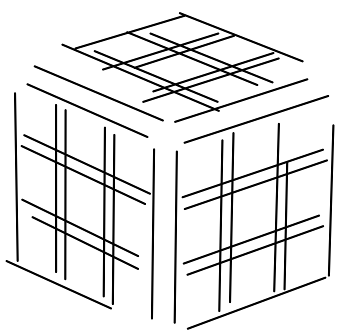

c

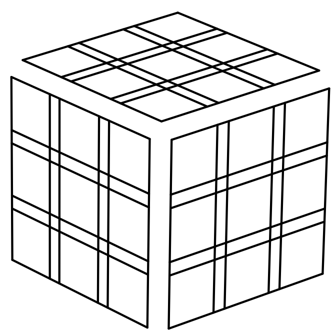

d

Figure 7: Camera parameter computation: (a) calibration cube (b) edges extracted (c) lines fitted (d) internal cube model.

The overall sequence of steps involved in pre-calibrating the system is thus fairly simple. With the turntable rotating, a sequence of images without any objects is taken. This memorizes the default background and the location of the binary code. A reference model is then placed on the turntable and the camera position automatically determined (currently we use the shape and position of the turntable top). This last stage could conceivably be replaced by a set of calibration points permanently fixed to the turntable. The result is a system that can be operated by a naïve user such as a CAD designer or graphics artist.

8 Real image results

We have tested our algorithm on a number of real image sequences. Figure 5 shows a sample image of a cup sitting on the turntable. Applying the adaptation and classification techniques described previously, we obtain the thresholded image shown in Figure 6. For this image sequence, it was necessary to lower the thresholds in the bright white areas of the adaptation image, because the shadows cast by the cup were causing an incorrect classification (most of the turntable top would be classified as part of the object). As we can see from the thresholded image, the algorithm still misclassifies isolated background pixels as foreground. Conversely, some of the specularities on the cup have been misclassified as background. Using a small amount of propagation and shrinking [Rosenfeld and Kak, 1976] should help remove these problems. A better long-term solution would be to use color images, since there is less chance of confusion, and since shaded regions (going from dark to light) are not forced to cross the background color.

Figure 8 shows the final model constructed from the cup image sequence. The final reconstruction captures the overall shape of the cup quite well. The major source of errors in the reconstruction is due to the specularities that cause erroneous gray nodes in the middle of the model (these are not visible in Figure 8, which renders gray nodes at the lowest level as opaque).

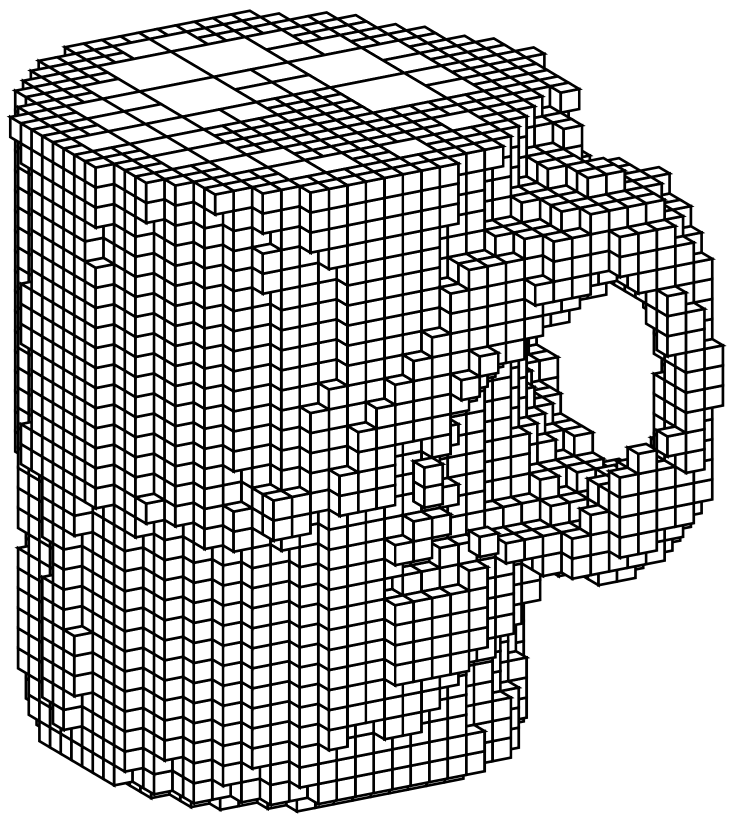

Figure 8: Octree model derived from real cup images

9 Extensions

There are a number of efficiency optimizations that could be added to our algorithm. To reduce the cost of the cube corner projections, there are several techniques that we could use:

1. cache the projections, since each corner is usually used more than once;
2. project only one corner, and used fixed vectors to define the other seven corners;
3. use recursive subdivision of the projected octree cubes to obtain the image coordinates of the points at the desired resolution.

Note that these last two approaches do not generate the exact corner positions, but this is perfectly acceptable, so long as a larger bounding box results.

We could further reduce the number of cubes projected by examining only visible cubes. This would remove from consideration both the cubes on the back side of the object and also those interior to the object (cubes that are not on the surface). It would then only be possible to remove a single layer of cubes at a time, and a hole in the object would require several views to "eat its way through" the object.

Adding gray level or color mapping onto the cubes in the octree would enhance the realism of the reconstruction. However, this is not an easy task, since many different intensities could map to a single cube, both within a single frame and between frames [Potmesil, 1987]. We could also use this stage to check for inconsistencies, such as white cubes that become visible later on.

Our octree construction algorithm would be more powerful if we could change the position of the camera and/or the object. The former case is easier to handle. We simply re-calibrate the system, and continue processing with the new camera parameters (we could also use more than one camera simultaneously). An interesting empirical question is whether we should still use the same hierarchical strategy as before (coarse to fine refinement), or whether we should process just the finest level—or maybe even the whole tree—for each new silhouette. The pure hierarchical algorithm described in this paper could then be replaced with a more flexible control strategy, which would decide how many whole or part levels to process depending on the real-time constraints imposed by the rate of incoming images.

The change in object orientation caused by repositioning it on the turntable is also simple to handle if the object motion is known. In this case, we can transform the octree to its new orientation [Ahuja and Nash, 1984; Weng and Ahuja, 1987] and continue processing as before. An example of such a known transformation would be if the object had only a few stable poses. Determining the object motion from the volumetric data itself is more difficult [Chien and Aggarwal, 1986a], especially when both the old and new object models contain areas that are extraneous. This remains an interesting area of future research.

One final interesting area of research is the interaction between the bounding volume generated by this algorithm and the deformable surface model computed from optic flow [Szeliski, 1990]. In this complementary approach to shape from rotation, knowledge of the optic flow and object motion provides a sparse and somewhat noisy estimate of points on the object's surface which are integrated using an elastic surface model. The bounding volume described by the octree can certainly provide inequality constraints on the deformable model, but can it also provide unambiguous surface positions in certain cases? Each ray from the camera passing through a pixel inside the silhouette must hit something opaque inside at least one of the black cubes in its path. In the general case, this *occupancy constraint* is complicated to represent and use. A more practical approach is to track the silhouette over three or more frames to estimate the location and curvature of points on the surface of the object [Giblin and Weiss, 1987; Vaillant, 1990].

10 Discussion

Given the current performance of our algorithm, is it fair to call it a "real-time" method? The microwave turntable that we use to rotate our object turns at 0.5 revolutions per minute. The time to acquire, process, and display a 512×480 image on our workstation is about 1.7 seconds per frame for adaptation and thresholding, and 3.0 seconds for an incremental octree construction step of moderate complexity (including the display of the current model). This means that we can process about 40 views per rotation, which is perfectly adequate for obtaining a bounding volume.

Ideally, we would like to speed up the turntable rotation (and the processing) by a factor of 10. This should be achievable with the next generation of faster RISC processors. Because our algorithm is essentially data parallel (both at the pixel and cube levels), it would be easy to obtain true real-time performance with a SIMD parallel machine.

A more important question might be: is our system useful and easy to use? Compared to previous octree construction algorithms, our new hierarchical approach requires less computation because it only examines those cubes close to the surface of the object. It provides a coarse model of the octree rapidly, which improves as the object continues to rotate in front of the camera. Compared to the alternatives of manually entering a model using a 3-D pointer or using structured light, our system is easier to use and requires less equipment. However, it still has the same limitation as previous silhouette-based algorithms, such as a limited precision and the inability to detect concavities in the object. To be truly useful, our method will have to be combined with more sophisticated shape from motion algorithms that track surface markings on the object. As part of such a shape from rotation system, it can quickly and automatically provide 3-D shape descriptions of real object for geometric modeling applications.

References

[Ahuja and Nash, 1984] N. Ahuja and C. Nash. Octree representation of moving objects. *Computer Vision, Graphics, and Image Processing*, 26:207–216, 1984.

[Ballard and Brown, 1982] D. H. Ballard and C. M. Brown. *Computer Vision*. Prentice-Hall, Englewood Cliffs, New Jersey, 1982.

[Caprile and Torre, 1990] B. Caprile and V. Torre. Using vanishing points for camera calibration. *International Journal of Computer Vision*, 4(2):127–139, March 1990.

[Carlbom *et al.*, 1985] I. Carlbom, I. Charkravarty, and D. Vanderschel. A hierarchical data structure for representing the spatial decomposition of 3-D objects. *IEEE Computer Graphics and Applications*, 5(4):24–31, 1985.

[Chen and Huang, 1988] H. H. Chen and T. S. Huang. A survey of construction and manipulation of octrees. *Computer Vision, Graphics, and Image Processing*, 43:409–431, 1988.

[Chien and Aggarwal, 1986a] C. H. Chien and J. K. Aggarwal. Identification of 3D objects from multiple silhouettes using quadtrees / octrees. *Computer Vision, Graphics, and Image Processing*, 36:256–273, 1986.

[Chien and Aggarwal, 1986b] C. H. Chien and J. K. Aggarwal. Volume/surface octrees for the representation of three-dimensional objects. *Computer Vision, Graphics, and Image Processing*, 36:100–113, 1986.

[Chien *et al.*, 1988] C. H. Chien, Y. B. Sim, and J. K. Aggarwal. Generation of volume/surface octree from range data. In *IEEE Computer Society Conference on Computer Vision and Pattern Recognition (CVPR'88)*, pages 254–260, IEEE Computer Society Press, Ann Arbor, Michigan, June 1988.

[Clark, 1982] J. H. Clark. The geometry engine: a VLSI geometry system from graphics. *Computer Graphics (SIGGRAPH'87)*, 16(3):65–72, June 1982.

[Giblin and Weiss, 1987] P. Giblin and R. Weiss. Reconstruction of surfaces from profiles. In *First International Conference on Computer Vision (ICCV'87)*, pages 136–144, IEEE Computer Society Press, London, England, June 1987.

[Hong and Shneier, 1985] T.-H. Hong and M. O. Shneier. Describing a robot's workspace using a sequence of views from a moving camera. *IEEE Transactions on Pattern Analysis and Machine Intelligence*, PAMI-7(6):721–726, November 1985.

[Jackins and Tanimoto, 1980] C. L. Jackins and S. L. Tanimoto. Oct-trees and their use in representing three-dimensional objects. *Computer Graphics, and Image Processing*, 14:249–270, 1980.

[Martin and Aggarwal, 1983] W. N. Martin and J. K. Aggarwal. Volumetric description of objects from multiple views. *IEEE Transactions on Pattern Analysis and Machine Intelligence*, PAMI-5(2):150–158, March 1983.

[Matthies *et al.*, 1989] L. H. Matthies, T. Kanade, and R. Szeliski. Kalman filter-based algorithms for estimating depth from image sequences. *International Journal of Computer Vision*, 3:209–236, 1989.

[Meagher, 1982] D. Meagher. Geometric modeling using octree encoding. *Computer Graphics, and Image Processing*, 19:129–147, 1982.

[Noborio *et al.*, 1988] H. Noborio, S. Fukada, and S. Arimoto. Construction of the octree approximating three-dimensional objects by using multiple views. *IEEE Transactions on Pattern Analysis and Machine Intelligence*, PAMI-10(6):769–782, November 1988.

[Pentland, 1986] A. P. Pentland. Perceptual organization and the representation of natural form. *Artificial Intelligence*, 28(3):293–331, May 1986.

[Potmesil, 1987] M. Potmesil. Generating octree models of 3D objects from their silhouettes in a sequence of images. *Computer Vision, Graphics, and Image Processing*, 40:1–29, 1987.

[Rosenfeld and Kak, 1976] A. Rosenfeld and A. C. Kak. *Digital Picture Processing*. Academic Press, New York, New York, 1976.

[Samet, 1989] H. Samet. *The Design and Analysis of Spatial Data Structures*. Addison-Wesley, Reading, Massachusetts, 1989.

[Sawhney *et al.*, 1990] H. S. Sawhney, J. Oliensis, and A. R. Hanson. Description and reconstruction from image trajectories of rotational motion. In *Third International Conference on Computer Vision (ICCV'90)*, pages 494–498, IEEE Computer Society Press, Osaka, Japan, December 1990.

[Solina and Bajcsy, 1990] F. Solina and R. Bajcsy. Recovery of parametric models from range images: the case for superquadrics with global deformations. *IEEE Transactions on Pattern Analysis and Machine Intelligence*, 12(2):131–147, February 1990.

[Srivastava and Ahuja, 1990] S. K. Srivastava and N. Ahuja. Octree generation from object silhouettes in perspective views. *Computer Vision, Graphics, and Image Processing*, 49:68–84, 1990.

[Szeliski, 1990] R. Szeliski. *Shape from Rotation*. Technical Report 90/13, Digital Equipment Corporation, Cambridge Research Lab, December 1990. For ordering information, please send a message to techreports@crl.dec.com with the word `help` in the Subject line.

[Vaillant, 1990] R. Vaillant. Using occluding contours for 3D object modeling. In *First European Conference on Computer Vision (ECCV'90)*, pages 454–464, Springer-Verlag, Antibes, France, April 23–27 1990.

[Veenstra and Ahuja, 1986] J. Veenstra and N. Ahuja. Efficient octree generation from silhouettes. In *IEEE Computer Society Conference on Computer Vision and Pattern Recognition (CVPR'86)*, pages 537–542, IEEE Computer Society Press, Miami Beach, Florida, June 1986.

[Weng and Ahuja, 1987] J. Weng and N. Ahuja. Octree of objects in arbitrary motion:

representation and efficiency. *Computer Vision, Graphics, and Image Processing*, 39:167–185, 1987.

A Serial and parallel half-distance transforms

Our octree construction algorithm uses the half-distance transform to test the bounding boxes of projected cubes against the silhouette images. The half-distance transform is a one-sided version of the chessboard distance transform [Rosenfeld and Kak, 1976]. Given a binary image, it computes for each pixel the size of the largest all ones square starting at that pixel.

The serial version of the algorithm computes

$$f^{(1)}(i,j) = \min(f^{(0)}(i,j), 1 + \min_{(u,v)\in N_3} f^{(1)}(i+u, j+v))$$

in reverse raster order, where $f^{(0)}(i,j)$ is the input binary image, and $N_3 = \{(0,1),(1,0),(1,1)\}$. A simple parallel version of the algorithm can be drived from the PD algorithm described in [Rosenfeld and Kak, 1976, p. 356]

$$f^{(m+1)}(i,j) = f^{(0)}(i,j) + \min_{(u,v)\in N_4} f^{(m)}(i+u, j+v),$$

where $N_4 = \{(0,0),(0,1),(1,0),(1,1)\}$. This algorithm takes d steps to converge, where d is the diameter of the largest region (the maximum value in the distance map). A variant on this algorithm is

$$f^{(m+1)}(i,j) = \min(f^{(m)}(i,j), 1 + \min_{(u,v)\in N_3} f^{(m)}(i+u, j+v)),$$

where initially $f^{(0)}(i,j)$ are set to 0 or ∞ for pixels outside/inside the silhouette.

A quicker version of the preceding parallel algorithm uses $2\log d$ steps

$$\begin{aligned} f^{(2m+1)}(i,j) &= \min(f^{(2m)}(i,j), s + \min_{(u,v)\in N_2} f^{(2m)}(i+su, j+sv)) \\ f^{(2m+2)}(i,j) &= \min(f^{(2m+1)}(i,j), s + f^{(2m+1)}(i+s, j+s)), \end{aligned}$$

where $s = 2^m$ and $N_2 = \{(0,1),(1,0)\}$. This algorithm doubles the distance to the neighbors every two iterations.

If the number of parallel processor available is less than the number of pixels—for example when using a MIMD machine or a smaller SIMD array—it pays to reduce the total amount of computation performed. In this case, we can use a hierarchical version of the parallel half-distance algorithm. We use the following pyramidal algorithm

$$\begin{aligned} f^{(2m+1)}(s_x i, s_y j) &= \min(f^{(2m)}(s_x i, s_y j), s + \min_{(u,v)\in N_2} f^{(2m)}(s_x i + su, s_y j + sv)) \\ f^{(2m+2)}(s_x i, s_y j) &= \min(f^{(2m+1)}(s_x i, s_y j), s + f^{(2m+1)}(s_x i + s, s_y j + s)) \end{aligned}$$

in two fine-to-coarse-to-fine sweeps. In the first sweep, $s_y = 1$, and $s_x = s = 2^m$ going up the pyramid and $s_x = s = 2^{(2M-m)}$ going down, where $M = \log_2 d$ is the height of the pyramid. In the second sweep, the roles of s_x and s_y are reversed. This algorithm first propagates the distances horizontally and diagonally, subsampling the points by 2 horizontally. The algorithm then repeats the procedure subsampling vertically. Because the number of points being updated is reduced by 2 every 2 steps, the total number of operations is $O(n)$.

B Templates for Gray coded positioning ring and calibration cube

Figures 9 and 10 show the patterns used for the 8-bit turntable position encoding ring (suitable for the 9” *mini* MICRO-GO-ROUND®turntable) and the $4'' \times 4''$ calibration cube. Both figures show the patterns at half scale. Full scale versions of these figures can be extracted from the PostScript version of this report. For information on how to obtain an electronic copy of this document, please send a message to `techreports@crl.dec.com` with the word `help` in the Subject line.

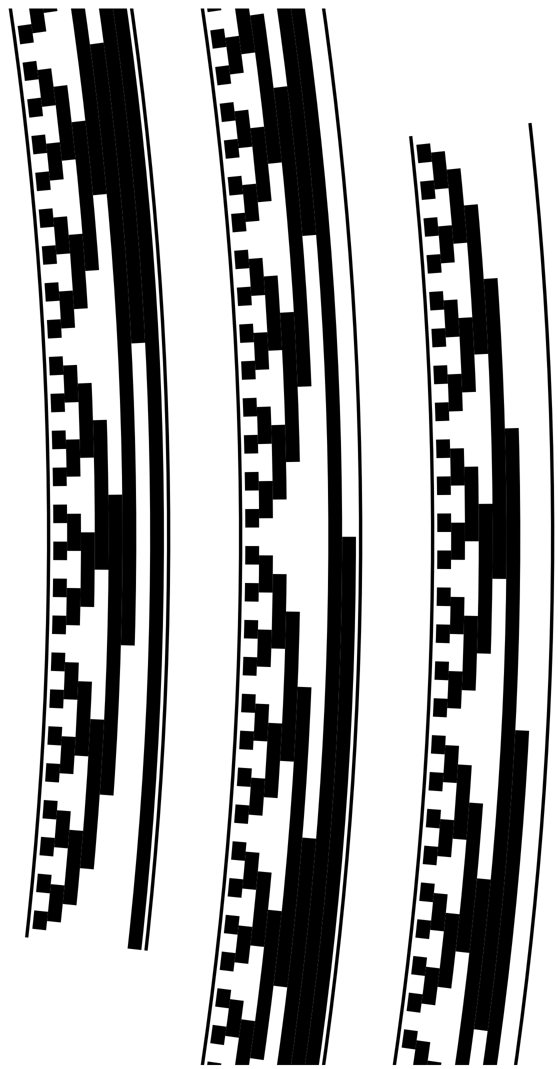

Figure 9: Turntable orientation ring with binary Gray code (1/2 scale).

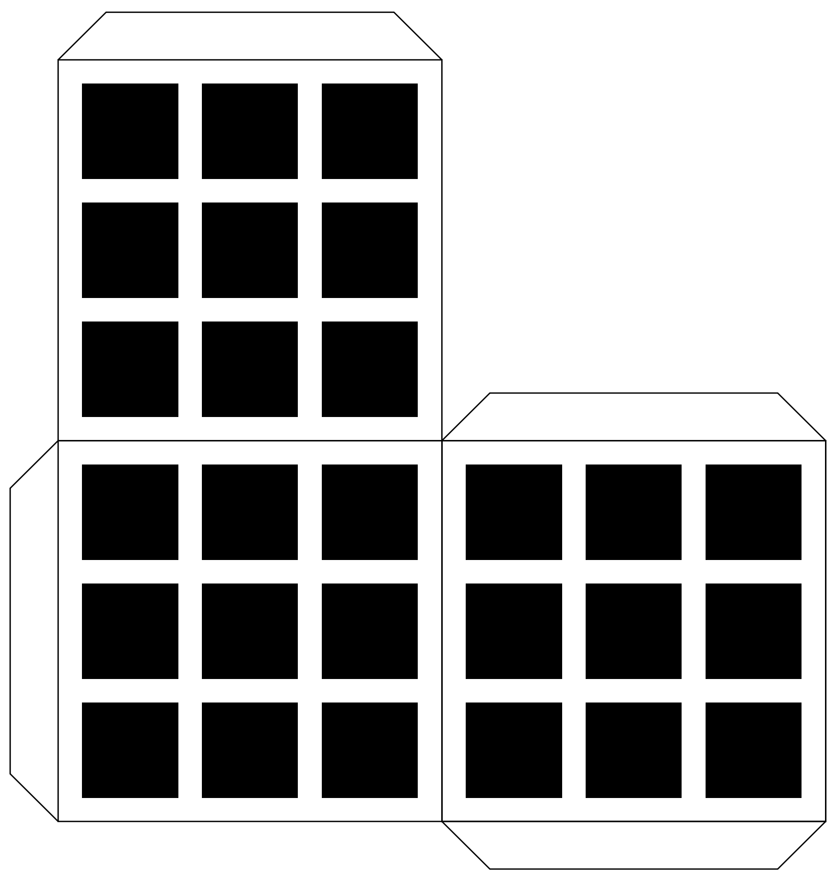

Figure 10: Pattern for calibration cube ($^1/_2$ scale).